Int. J. Electrochem. Sci., 10 **(2015)** 3859 - 3866

International Journal of
ELECTROCHEMICAL
SCIENCE
www.electrochemsci.org

Short Communication

A Facile Approach for Preparing MnO_2-Graphene Composite as Anode Material for Lithium-Ion Batteries

Kang Wen[1], *Guanghui Chen*[2], *Feng Jiang*[1], *Xiangyang Zhou*[2,*], *Juan Yang*[2]

[1] School of Materials Science and Engineering, Central South University, Changsha 410083, China
[2] School of Metallurgy and Environment, Central South University, Changsha 410083, China
[*]E-mail: hncsyjy308@163.com

Received: 27 January 2015 / *Accepted:* 2 March 2015 / *Published:* 23 March 2015

A facile method to prepare the MnO_2-graphene composite was proposed. The composite with a sandwich structure was synthesized by oxidizing part of the carbon atoms in the framework of graphene. By using graphene as buffer carrier, MnO_2 was homogeneously coated onto the surface of graphene. Electrochemical properties of this MnO_2-graphene composite were characterized and it exhibits excellent cyclic stability and good rate properties. The MnO_2-graphene electrode retains a capacity of 752 mA h g^{-1} at a current density of 100 mA g^{-1} after 65 cycles, making it a promising anode material for lithium ion batteries.

Keywords: MnO_2, graphene, composite, lithium ion batteries, oxidation

1. INTRODUCTION

Due to the depletion of fossil fuels and increasing environmental problems, great efforts have been made to develop novel electrochemical systems for energy storage and conversion [1, 2]. Lithium ion batteries (LIBs) are considered to be one of the most practical and effective technologies for energy storage and conversion [3, 4]. Therefore, developing the next generation LIBs with high energy density, high power density and excellent cycling performance becomes critical [5]. In the last several years, great efforts have been made to develop new electrode materials to satisfy these demands [3, 6], and MnO_2 was considered to be a promising electrode material for LIBs due to its high theoretical capacity (1230mAh g^{-1}), low cost, environmental friendliness and natural abundance [7-9]. However, the low actual capacity and the poor cyclability of MnO_2 due to its large volume expansion and aggregation during Li insertion/extraction hindered its practical application [10-12]. As is well-known,

an effective way to solve these problems is to fabricate hybrid electrode materials that incorporated MnO_2 onto electrically conductive carbon materials [13, 14] or conducting polymers [15-17].

Graphene, a two-dimensional carbon material, is an ideal matrix for growing and anchoring nanomaterials for energy storage due to its superior electrical conductivity, high surface-to-volume ratio, ultrathin thickness, structural flexibility, and chemical stability [18, 19]. In recent reports, the MnO_2/graphene nanocomposites used as electrode materials for supercapacitors have been synthesized by using different methods [20-22]. In this work, a unique hierarchical structure was designed and the MnO_2-graphene composite was synthesized by oxidizing part of the carbon atoms in the framework of graphene.

A facile approach for preparing the MnO_2-graphene composite was presented in this paper. The MnO_2-graphene composite exhibited a sandwiched structure, and MnO_2 were well anchored onto the surface of graphene and incorporated between the layers. Meanwhile, as anode materials for lithium ion batteries, electrochemical performances of the MnO_2-graphene composite were characterized by cyclic voltammetry (CV) and galvanostatic charge-discharge tests.

2. EXPERIMENTAL

2.1 Synthesis of pure MnO_2 and MnO_2-graphene composite

Graphite oxide was prepared by Hummers method [23]. The as-prepared graphite oxide suspension was then dispersed in water to create a 0.05 wt.% dispersion. Exfoliation of graphite oxide to graphene oxide (GO) was achieved by ultrasonication of the dispersion for 120 min. The obtained brown dispersion was then subjected to 30 min of centrifugation at 3000 rpm to remove unexfoliated graphite oxide. In a typical procedure for chemical conversion of graphite oxide to graphene, the resulting homogeneous dispersion (200ml) was mixed with a given amount of hydrazine solution and 1.4 ml of ammonia solution (28 wt.% in water) in a 250 ml conical flask. The mass ratio of hydrazine to GO was about 7:10. After being vigorously stirred for a few minutes, the flask was then put in a water bath (95℃) for 1 h [24].

The procedure for synthesizing the MnO_2-graphene composite was illustrated in Fig.1. First, 300 mg $KMnO_4$ was added into the above suspension and the mixed solution was stirred with a stirring bar for 3h at 80℃. In this process, nanocrystalline MnO_2 formed on the surface of graphene framework due to the redox reaction [25, 26] shown as follows:

$$4KMnO_4 + 3C + H_2O \rightarrow 4MnO_2 + K_2CO_3 + 2KHCO_3 \quad (1)$$

After this, the produced sample was collected by filtration and should be washed several times with deionized water. The final MnO_2-graphene product was dried at 80 ℃ in a vacuum oven for 12 h.

For the preparation of MnO_2 powders, 300mg $KMnO_4$ and 0.2 ml H_2SO_4 (95%) were mixed with 25ml deionized water to form precursor. Then the precursor solution was transferred into a Teflon-sealed autoclave to carry out hydrothermal treatment at 150℃ for 4h [27].

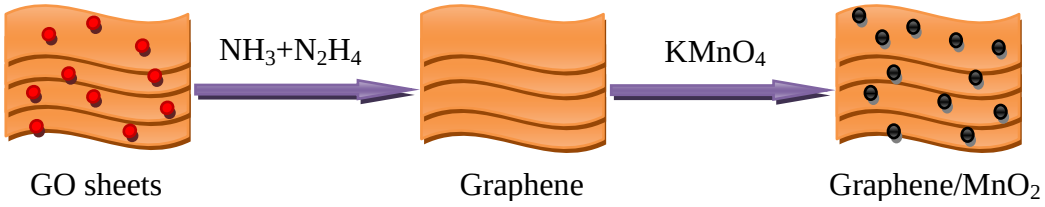

Figure 1. Schematic diagram for preparation of MnO_2-graphene composite

2.2 Characterization

Raman spectra of samples were recorded on a LabRAM HR800 spectrometer. Phases in MnO_2-graphene composite were identified by using X-ray powder diffraction (XRD, Rigaku-TTRIII with Cu Kα radiation). The morphologies of as-obtained samples were observed on a scanning electron microscopy (SEM, JSM-6360LV) and transmission electron microscope (TEM, JEM-2100). The content of interlayer water and MnO_2 in the composite was determined by adopting thermogravimetric analysis (TGA, SDTQ 600).

2.3 Electrochemical measurement

The test electrodes consisted of the active materials (80 wt.%), acetylene black (10 wt.%) and polyvinlidene difuoride (10 wt.%). The mixture was dissolved in N-methyl-2-pyrrolidene (NMP) under stirring to form slurry. Then the slurry was coated onto a copper foil substrate and dried in a vacuum oven for 12h at 120℃. Electrochemical tests were performed using CR2025 coin-type cells with lithium metal foils as the counter electrode. A solution of 1M $LiPF_6$ in ethylene carbonate /dimethyl carbonate (volume ratio of EC:DMC was 1:1) was used as the electrolyte， and the separator was Polypropylene membrane (Celgard-2400). The cells were charged and discharged under constant current within the voltage range from 0.01 to 3 V vs. Li/Li^+ on LAND batteries tester (CT-2001A, Wuhan Jinnuo Electron Co. Ltd.). Cyclic voltammetry (CV) tests were carried out on an electrochemical workstation (CHI660, China).

3. RESULTS AND DISCUSSION

Figure.2 shows a typical XRD pattern of the as-prepared MnO_2-graphene composite. Apart from the peaks of graphene, three broad peaks centered at 12°, 37°, and 66° are observed. These peaks can be indexed to α-MnO_2 (JCPDS file no. 42–1169), including its amorphous phase.

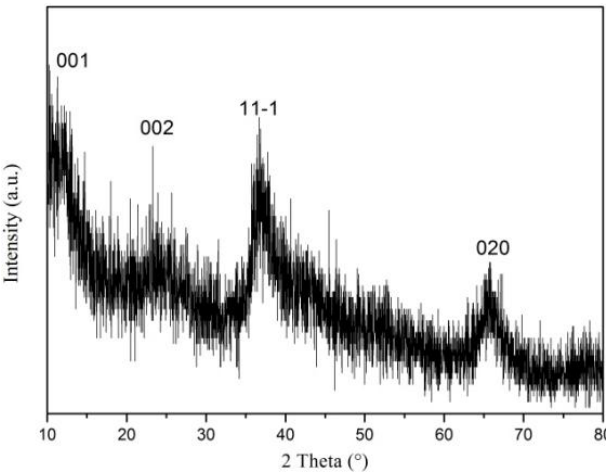

Figure 2. XRD pattern of the MnO_2-graphene composite

Raman spectroscopy is useful for analyzing the structure of inorganic materials with poor crystallinity [2]. As shown in Figure.3, two obvious peaks can be observed at 1590cm^{-1} and 1350cm^{-1} in the Raman spectrum of graphene, and this can be assigned to the G and D bands of graphene [28]. In Raman spectra of pure MnO_2 and MnO_2-graphene composite, the peaks at around 640cm^{-1} are in good agreement with the Raman feature of birnessite-type MnO_2 compounds reported before [29], which can be viewed as the symmetric stretching vibration (Mn-O) of the MnO_6 groups [30]. In the Raman spectrum of MnO_2-graphene composite, the intensity of graphene peaks decreased as the reaction described in equation (1) occurred，indicating the replacement of carbon atoms by MnO_2 in the framework of graphene.

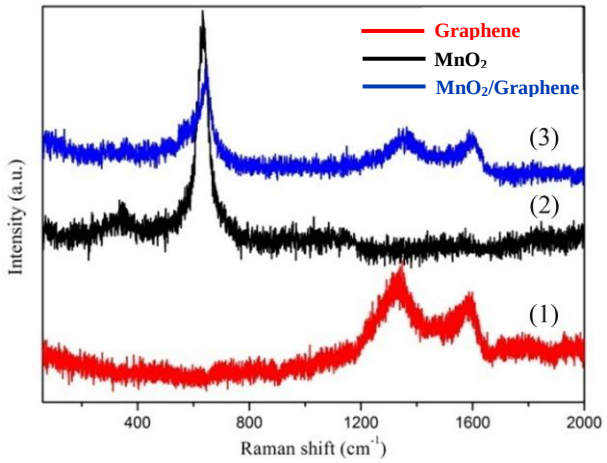

Figure 3. Raman spectra of (1) graphene, (2) MnO_2, and (3) MnO_2-graphene composite

TGA curves of the as-prepared MnO_2-graphene composite is shown in Figure.4. The MnO_2-graphene composite exhibits obvious weight loss from 25 to 1000 °C. The 16.6 % weight loss between 25 and 150 °C could be attributed to the liberation of adsorbed water in composites. An additional 37%

weight loss between 300 and 450 °C corresponds to the loss of graphene [27]. Therefore, the content of MnO_2 in the MnO_2-graphene composite is 46.4 %.

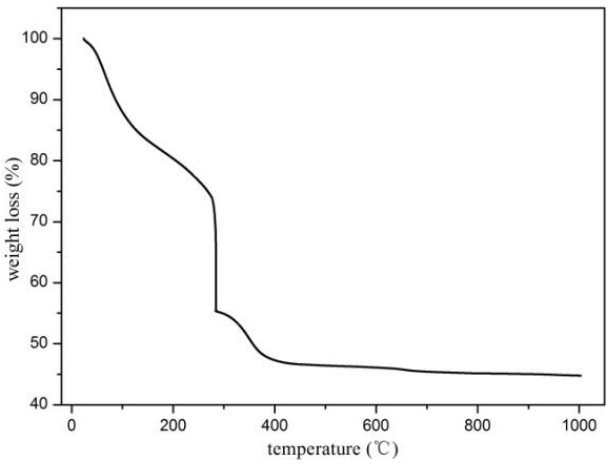

Figure 4. TGA curve of the MnO_2-graphene composite

Figure.5a shows the typical morphology of the MnO_2-graphene composite. It can be seen that MnO_2 particles existed on the surface of graphene, and the composites exhibit clear lamellar structure. The large surface area of graphene enabled sufficient interaction between MnO_2 nanoparticles and graphene, facilitating the formation of sandwich structures. Figure.5b is the TEM image of MnO_2-graphene composite. It can be seen that the MnO_2 nanoparticles was attached on the surface of graphene or sandwiched between the layers, and the graphene served as supporter and electrically medium [31]. The surface of graphene was decorated randomly with MnO_2 nanoparticles. The excellent flexibility of graphene and the sandwich structure of this composite could effectively buffer the volume expansion of MnO_2 during the charge/discharge process. In addition, graphene in the composite act as not only lithium storage electrode but also good conductive medium to facilitate the electron transportation. Large surface areas of graphene sheets and MnO_2 nanoparticles provide sufficient areas for interactions between electrode and electrolyte. Moreover, MnO_2 nanoparticles on the surfaces of graphene could also prevent the stack of graphene sheets. In summary, due to the synergistic effects of MnO_2 nanoparticles and graphene, this composite exhibited high electrical conductivity and excellent electrochemical performance.

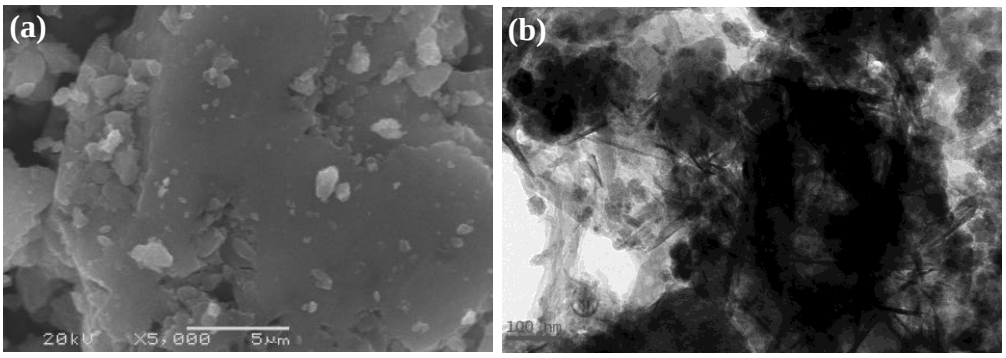

Figure 5. (a) SEM and (b) TEM images of MnO_2-graphene composite

Figure.6 shows the cyclic voltammetry curves and the first three galvanostatic charge-discharge profiles of MnO_2-graphene composite electrode between 0.01 V and 3 V at a scanning rate of 1 mV s^{-1}. The CV curves presented in Figure.6a clearly showed the redox peaks corresponding to the intercalation and deintercalation of Li ions into/from the MnO_2-graphene electrode. During the first negative scan, a cathodic peak appeared at 0.55V, corresponding to the formation of a solid electrolyte interphase (SEI) layer. This peak disappeared after the first cycle, demonstrating that the SEI formation mainly occurs in the first cycle. Two oxidation peaks at 1.3V and 2.1V can also be observed in the curves，indicating the two-step electrochemical oxidation of Mn^0 to Mn^{4+}. In agreement with the CV results, two voltage plateaus can be observed during the charge process. However, there was only one plateau in the discharge process, demonstrating the reduction reaction of MnO_2 with Li ions in one step. The reaction between MnO_2 and Li can be described as follows [32, 33]：

$$MnO_2 + 4Li + 4e^- \rightleftharpoons 2Li_2O + Mn \qquad (2)$$

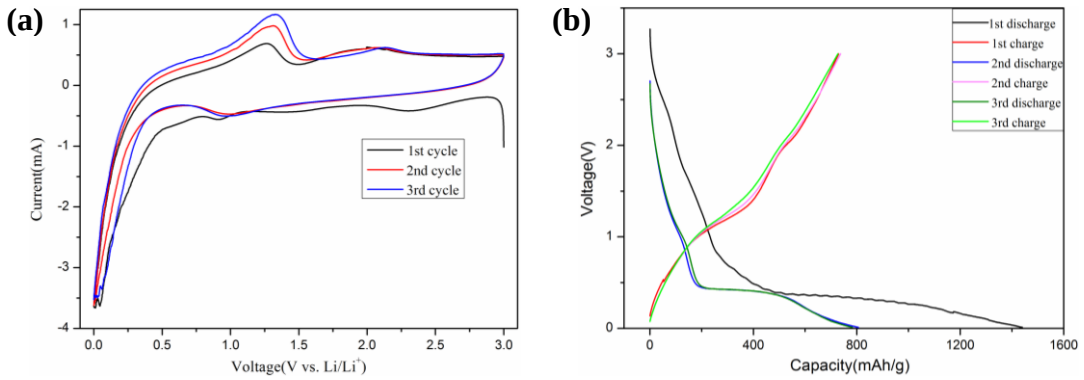

Figure 6. (a) Cyclic voltammetry curves and (b) the first three charge-discharge profiles of MnO_2-graphene electrode between 0.01V and 3V at a current density of 100 mA g^{-1}

The first discharge and charge capacities are 1589 and 746 mAh g^{-1}, respectively, with a coulumbic efficiency of 47％. It should be noted that the discharge capacity for the first cycle of MnO_2-graphene electrode is much higher than the theoretical value of pure MnO_2 (1230 mAh g^{-1}). This could be attributed to the irreversible reactions of electrodes，i.e. the formation of solid electrolyte interphase (SEI) layer on the surface of electrode due to the decomposition of electrolyte [34].

Figure.7 shows the cycling performance and rate capability of the MnO_2-graphene composite electrode at a current density of 100mA g^{-1}. It can be seen that the MnO_2-graphene electrode exhibits good cycling stability, and there is no obvious capacity decay after the first cycle. The coulombic efficiency of the MnO_2-graphene electrode was maintained over 95% (except for the first 3 cycles), and this is probably ascribed to the stable sandwich structure of MnO_2-graphene composite. The graphene encapsulation enhanced interaction between MnO_2 and graphene, and also hindered direct contact between MnO_2 and the electrolyte. As the cycling test proceeded, the materials which was wrapped inside become electrochemically active as they come into contact with the electrolyte [35].

To evaluate the rate capability of MnO_2-graphene composite electrode, cells were cycled at stepped current densities of 0.1A/g, 0.2A/g, 0.4A/g and 0.8A/g. As shown in Figure.7b, at a current

density of 0.1A/g, the MnO_2-graphene electrode exhibited better electrochemical performance in the first 55 cycles. When the current densities ascended to 0.2A/g, 0.4A/g and 0.8A/g, the capacities dropped to 581.7 mAh g^{-1}, 410.5 mAh g^{-1} and 304.5 mAh g^{-1}, respectively. When the current density was dropped back to 0.1A/g, the capacity could be recovered to 686 mAh g^{-1}, demonstrating an excellent electrochemical reversibility of the MnO_2-graphene electrode.

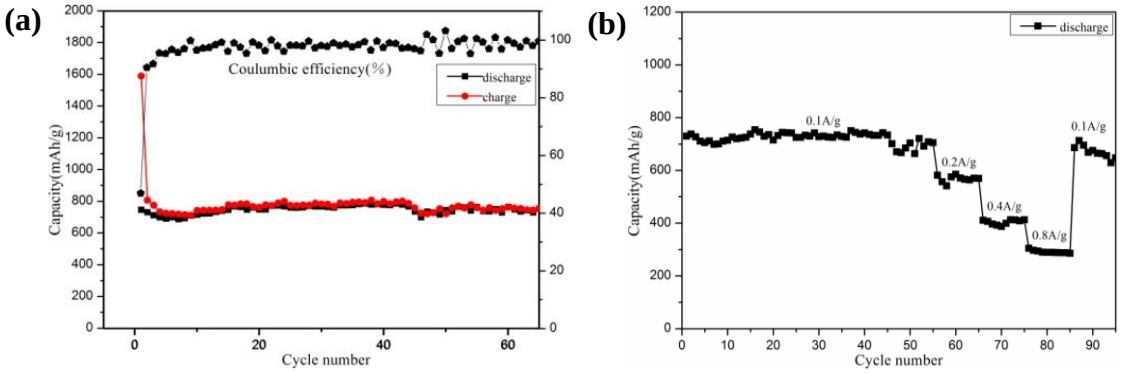

Figure 7. (a) Cycling performance and (b) Rate capability curves of the MnO_2-graphene composite electrode at a current density of 100 mA g^{-1}

4. CONCLUSIONS

A facile approach to synthesized a sandwich-structured MnO_2-graphene composite was developed in this study. Characterization methods such as Raman spectroscopy, SEM and TEM were used to demonstrate that MnO_2 nanoparticles were well anchored on the surface of graphene and sandwiched between the layers. The electrochemical tests results showed that the MnO_2-graphene composite exhibits a high initial capacity of 746 mAh g^{-1} at a current density of 100 mA g^{-1}, and retained a capacity of 752 mAh g^{-1} after 65 cycles. With the improved electrochemical performance, the nanocomposite could be a promising electrode material for lithium-ion batteries.

ACKNOWLEDGEMENT
This study was supported by the National Natural Science Foundation of China (51274240, 51204209).

References

1. H. Huang and X. Wang, *Phys. Chem. Chem. Phys*., 15 (2013) 10367
2. H. Huang and X. Wang, *Nanoscale*, 3 (2011) 3185
3. Y. Su, S. Li, D. Wu, F. Zhang, H. Liang, P. Gao, C. Cheng and X. Feng, *ACS Nano*, 6 (2012) 8349
4. V. Etacheri, R. Marom, R. Elazari, G. Salitra and D. Aurbach, *Energy Environ. Sci*., 4 (2011) 3243
5. L. Li, A. O. Raji and J. M. Tour, *Adv. Mater*., 25 (2013) 6298

6. G. Zhou, J. Wang, P. Gao, X. Yang, Y. He, X. Liao, J. Yang and Z. Ma, *Ind. Eng. Chem. Res*., 52 (2013) 1197
7. H. Lai, J. Li, Z. Chen and Z. Huang, *ACS Appl. Mater. Interfaces*, 4 (2012) 2325
8. A. Yu, H. W. Park, A. Davies, D. C Higgins, Z. Chen and X. Xiao, *J. Phys. Chem. Lett*., 2 (2011) 1855
9. L. Shao, J. Shu, R. Ma, M. Shui, L. Hou, K. Wu, D. Wang and Y. Ren, *Int. J. Electrochem. Sci*., 8 (2013) 1170
10. Q. Li, Z. Wang, G. Li, R. Guo, L. Ding and Y. Tong, *Nano Lett*., 12 (2012) 3803
11. A. E. Fischer, K. A. Pettigrew, D. R. Rolison, R. M. Stroud and J. W. Long, *Nano Lett*., 7 (2007) 281
12. W. Yao, J. Yang, J. Wang and L. Tao, *Electrochim. Acta*, 53 (2008) 7326
13. S. W. Lee, J. Kim, S. Chen, P. T. Hammond and Y. Shao-Horn, *ACS Nano*, 4 (2010) 3889
14. Z. Lei, F. Shi and L. Lu, *ACS Appl. Mater. Interfaces*, 4 (2012) 1058
15. J. Zhang, J. Jiang and X. Zhao, *J. Phys. Chem*. C, 115 (2011) 6448
16. Z. Li, J. Wang, Z. Wang, L. Niu, J. Sun and S. Yang, *J. Chin. Chem. Soc*., 59 (2012) 1351
17. R. Liu and S. B. Lee, *J. Am. Chem. Soc*., 130 (2008) 2942
18. K. S. Novoselov, A. K. Geim, S. V. Morozov, D. Jiang, Y. Zhang, S. V. Dubonos, I. V. Grigorieva and A. A. Firsov, *Science*, 306 (2004) 666
19. A. K. Geim, *Science*, 324 (2009) 1530
20. Z. Wu, W. Ren, D. Wang, F. Li, B. Liu and H. Cheng, *ACS Nano*, 4 (2010) 5835
21. Y. Li, N. Zhao, C. Shi, E. Liu and C. He, *J. Phys. Chem*. C, 116 (2012) 25226
22. F. Tu, T. Wu, S. Liu, G. Jin and C. Pan, *Electrochim. Acta*, 106 (2013) 406
23. W. S. Hummers Jr. and R.E. Offeman, *J. Am. Chem. Soc*., 80 (1958) 1339
24. D. Li, M. B. Muller, S. Gilje, R. B. Kaner and G. G. Wallace, *Nat. Nanotechnol*., 3 (2008) 101
25. X. Jin, W. Zhou, S. Zhang and G. Z. Chen, *Small*, 3 (2007) 1513
26. W. Xiao, H. Xia, J. Y. H. Fuh and L. Lu, *Phys. Scr*., 139 (2010) 1
27. H. Xia, M. Lai and L. Lu, *J. Mater. Chem*., 20 (2010) 6896
28. C. Bao, L. Song, W. Xing, B. Yuan, C. A. Wilkie, J. Huang, Y. Guo and Y. Hu, *J. Mater. Chem*., 22 (2012) 6088
29. A. Ogata, S. Komaba, R. Baddour-Hadjean, J. P. Pereira-Ramos and N. Kumagai, *Electrochim. Acta*, 53 (2008) 3084
30. T. Gao, M. Glerup, F. Krumeich, R. Nesper, H. Fjellvåg and P. Norby, *J. Phys. Chem*. C, 112 (2008) 13134
31. Y. Yu, B. Zhang, Y. He, Z. Huang, S. W. Oh and J. K. Kim, *J. Mater. Chem*. A, 1 (2013) 1163
32. B Sun, Z. Chen, H. S. Kim, H. Ahn and G. Wang, *J. Power Sources*, 196 (2011) 3346
33. M. S. Wu, P. J. Chiang, J. T. Lee and J. C. Lin, *J. Phys. Chem*. B, 109 (2005) 23279
34. J. Liu, Y. Li, X. Huang, R. Ding, Y. Hu, J. Jiang and L. Liao, *J. Mater. Chem*., 19 (2009) 1859
35. L. Xiao, Y. Cao, J. Xiao, B. Schwenzer, M. H. Engelhard, L. V. Saraf, Z. Nie, G. J. Exarhos and J. Liu, *Adv. Mater*., 24 (2012) 1176